**ORIGINAL ARTICLE**

# Experimental Investigation of Noise and Vibration in a Multi-three Phase Unit Interior Permanent Magnet Synchronous Machine with Open-circuit Fault conditions

Sayyed Haleem Shah[1] · Xiaoyuan Wang[1] · Usman Abubakar[1] · Peng Gao[1]

## Abstract

Permanent magnet synchronous machines, especially interior permanent magnet (IPM) synchronous machines, are being used widely nowadays in a variety of applications. The (IPM) synchronous machine vibration and noise remain one of the critical factors to consider when some new design prototype of the machine is taken into consideration. In this paper, an efficient modular type fractional slot concentrated winding (FSCW) interior type permanent magnet synchronous motor (IPMSM) is designed, taking into account the capability of fault tolerance and open circuit fault conditions. The radial force and the associated vibration phenomenon are first investigated for the modular type (IPMSM) under normal operating conditions and then under symmetrical and asymmetrical three-phase units open circuit fault conditions. Two-dimensional (2-D) Fourier Transform has been used to investigate the relationship between the faulty operating conditions and the associated induced harmonics in the radial force density of the machine. Then, a detailed harmonic structural analysis, along with a three-dimensional (3-D) transient structural analysis, is performed on the stator of the proposed machine to investigate and verify the normal healthy design approach and the machine fault operating cases under post-fault conditions. Lastly, the vibration and noise characteristics of the prototype machine under the symmetrical and asymmetrical three-phase units' faulty conditions are thoroughly investigated for comparison purposes over a wide operating speed range. The findings from this comparative analysis are validated through experiments, which confirm the validation of the proposed design. Moreover, the associated considerations can be used by machine designers to lower the vibration and noise level in fault-tolerant modular design machines.

**Keywords** Permanent magnet synchronous motor · Electromagnetic force · Spectrum analysis · Electromagnetic vibration and noise · Fault-tolerance

✉ Peng Gao
gaopeng218@tju.edu.cn

Sayyed Haleem Shah
mian_shs@yahoo.com

Xiaoyuan Wang
xywang62@tju.edu.cn

Usman Abubakar
naallahabubakar@gmail.com

[1] School of Electrical and Information Engineering, Tianjin University, Tianjin, China

## 1 Introduction

Permanent magnet synchronous machines (PMSMs) with FSCW arrangements have recently been widely used in many application areas, including prominent ones like the automobile, the direct drive, and many other industrial applications. They are also used in electric vehicles requiring high power density electronics due to their standout advantages. Some of the main advantages of these types of machines are their high power density, high level of reliability, less vibration, and associated noise. It is also possible to rewind the modular PM machine into smaller three-phase components, each powered by a lower level inverter [1]. Moreover, they also receive more interest due to their low-level power and current requirements. The other standout advantage for this kind of modular design machine is its applications in industrial

and manufacturing processes requiring fault tolerance. Meanwhile, the modular type machine's vibration and noise performance analysis has not been investigated that much; therefore, it requires more attention as its vibrational force is directly connected to its noise level and overall stability. The main cause of the electromagnetic vibration and noise in an electric machine comprises the electromagnetic forces generated in an electric machine. Vibration and noise are caused due to electromagnetic forces interfacing with one another. Many scholars have performed research recently on the vibration, noise, and modal analysis of an electric motor. Lin et al. [2] Performed studies on the machine vibration phenomenon and have acknowledged that the air gap magnetic force acting on the stator teeth surfaces in an electric machine is the main source of electromagnetic vibration. Besnerais [3] Investigated that the machine cogging torque that varies with time and the machine radial forces have an important relationship with the slot and pole numbers and its least common multiple. Similarly, [4] calculated the radial electromagnetic force component using the Finite Element Analysis (FEA) technique. The calculated radial electromagnetic force included the zeroth-order components.

Some other research analysis that has been conducted recently to study the vibration and noise behavior of the standard three-phase machine includes the effect of magnetostriction on the vibration of the machine, along with its stress analysis [5]. Similarly, [6] investigates the effects of slots harmonics and the impact of machine loading on the machine's vibration. The effect of slot and pole numbers and their combination is studied in [7, 8] along with different winding layers configurations. Gan et al. [9] Discuss the skewing of stator slots and their effect on the vibration characteristics of an electric motor.

The traditional three-phase machine noise and vibration phenomenon have been investigated mostly under a standard three-phase winding design approach. The standard three-phase machine can have various other winding topologies and design methods based on the principles of conventional machines, such as the modular design machine, which are mostly used for fault-tolerant applications. Moreover, fault-tolerant machines are essential in modern industrial and aerospace applications. Henceforth, it is of extreme importance to investigate the vibration and noise response and the fault-tolerant capability of such machines when designed in a modular configuration for fault-tolerant applications, requiring the machine to work under hostile conditions. Publication [10] considers a modular design approach consisting of many dismountable units of the machine's stator. This kind of design approach is also followed in a five-phase in-wheel machine and some other machine designs [11–16].

In situations requiring high fault-tolerant reliability, the modular type (IPMSM) having multiple three-phase units may confront some severe faulty conditions like open circuit

faults in one or more three-phase units. Under such a case, the completely defective three-phase unit can be disconnected by switching off the power supply to that machine unit. Such three-phase unit faults can be divided into two main types: the symmetrical and asymmetrical open-circuit faults in a modular design multi three-phase machine. Henceforth, such operating conditions need more focus to understand the machine's vibration behavior under open-circuit fault situations.

This paper investigates the radial electromagnetic force density in a modular design multi three-phase units fractional slot interior permanent magnet synchronous machine and its associated vibration and noise phenomenon under different symmetrical and asymmetrical three-phase unit faults. This paper is comprised of 7 sections, with Sect. 2 describing the geometric structure and applied winding topology for the prototype machine. Section 3 describes open circuit faults in an electrical machine and its theoretical analysis. The performance analysis of the proposed machine under normal and fault operating conditions is discussed in Sect. 4. The structural, vibrational, and noise performance analysis of the machine under different three-phase units open circuit fault conditions are presented in detail in Sect. 5. Section 6 gives an experimental validation of the analyzed conditions, while a brief conclusion is presented in Sect. 7.

## 2 Modular Type Winding Topology and Prototype Machine Design

Figure 1a shows the standard three-phase winding design of an interior permanent magnet synchronous machine along with the modular type winding topology for the same machine shown in Fig. 1b. The given figures show that the mechanical structure for both machine designs is exactly the same; only the modular windings topology of one machine is different from the other, having its stator winding divided into different three-phase units. This prototype machine has
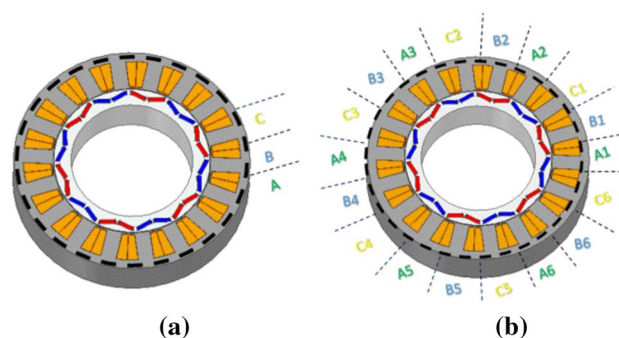


**Fig. 1** IPMSM machine design **a** Normal three-phase design **b** Modular type design

six three-phase units depending on the slot pole combinations with three slots and a pole pair making a single three-phase unit motor supplied by an independent three-phase inverter.

The machine phases for this kind of modular design machine do not have any overlapping (physical contact) with the other phases. Subsequently, the mutual coupling between the windings of the different phases is significantly lower than the ones for other distributed windings configurations of the prototype modular machine. This modular type machine design allows a reduction in the spread of faults inside the machine; simultaneously, it is extremely important to verify the efficiency and the radial force distribution of the machine under the normal healthy operating condition and faulty operating conditions. Table 1 presents parameters for the modular type design of the machine prototype and the normal three-phase machine design having the same dimensions but different winding configurations.

## 3 Open Circuit Faults and Their Theoretical Analysis

### 3.1 Magnetomotive Force and Open-circuit Faults

Open-circuit faults in an electrical machine can be of a simple nature like a single-phase fault or can be more complex. Still, always the theoretical analysis principles are based on a single-phase open-circuit fault. When a single or multiple phase fault occurs in a machine, it greatly changes the distribution of the magnetomotive force inside the machine. The modified magnetomotive force results in an electrical unbalance around the machine's circumference. The harmonic equation for the

**Table 1** Specifications of the prototype motor

| Parameters | Values | |
|---|---|---|
| | Regular design | Modular design |
| Rated power (kW) | 35 | |
| Rated speed (r/min) | 3600 | |
| Rated torque (N/m) | 93 | |
| Poles per slots | 12/18 | |
| Stator outer diameter (mm) | 300 | |
| Stator inner diameter (mm) | 200 | |
| Rotor diameter (mm) | 198.2 | |
| Stack length (mm) | 60 | |
| Number of magnets per pole | 2 | |
| Magnet Width (mm) | 20 | |
| Magnet thickness (mm) | 5 | |
| Winding method | Star | |
| Number of three-phase units | 1 | 6 |

calculation of the stator generated magnetomotive force in a three-phase machine is given below

$$f_s(\alpha, t) = \sum_{r=1}^{\infty} \left( f^{rd_k} \cos(\omega t - vp\alpha) \right) + (f^{rr_k} \cos(\omega t - vp\alpha))$$

(1)

Here from this equation, it can be seen that the $r_{th}$ harmonic has two components. The first one rotates in the positive direction, while the second one rotates in the negative direction. Here $r$ represents the harmonic order, while $f^{rd_k}$ and $f^{rr_k}$ represents the $r_{th}$ harmonic amplitudes of the (MMF) rotating in the forward and reverse direction, respectively. Pole pair number is represented by $p$, while $\alpha$ and $\omega$ represents the geometrical angle and the angular frequency of the input current, respectively. In normal operating conditions, the amplitudes of the harmonic orders in a symmetrical three-phase machine are given below, with no even order harmonics.

$$f^{rd_k} = f^{rr_k} = 0 v = 6r + 3 = 3, 9, 15, 21...$$

$$f^{rd_k} = \frac{3f^{rd_{k\sigma}}}{2}, f^{rr_k} = 0 v = 6r + 1 = 1, 7, 13, 19, ...$$

$$f^{rd_k} = 0, f^{rr_k} = \frac{3f^{rr_{k\sigma}}}{2v} = 6r - 1 = 5, 11, 17, 23, ...$$

(2)

In a situation when the prototype machine is composed of multi three-phase units, the machine (MMF) calculation technique is slightly different from the traditional three-phase technique. The single winding (MMF) calculation technique is used and then applied to all the machine windings. The following equation can calculate the stator (MMF) for a single coil winding.

$$f_s(\alpha, t) = \sum_{r=1}^{\infty} f^{rd_k} \cos(\omega t + \lambda - \vartheta_e) * \cos(r(\alpha - \alpha_n))$$

$$+ \sum_{r=1}^{\infty} f^{rr_k} \cos[(\omega t + \lambda + \vartheta_e) * \cos(r(\alpha - \alpha_n))$$

(3)

Here $f^{rd_k, rr_k}$ represents the amplitude of (MMF) harmonics of the stator winding, while $\lambda$ and $\omega$ represents the electrical and pulsation angle supplied to the machine. $\vartheta_e$ and $\alpha_n$ represents the electrical angle and the corresponding axis angle belonging to the generic coil n. When all the stator coils are taken into consideration, the total (MMF) for the whole stator windings consisting of N number of coils is given by

$$f_s(\alpha, t) = \sum_{n=1}^{N} \sum_{r=1}^{\infty} f^{rd_k} \cos(\omega t + \lambda - \vartheta_e) * \cos(r(\alpha - \alpha_n))$$

$$+ \sum_{n=1}^{N} \sum_{r=1}^{\infty} f^{rr_k} \cos[(\omega t + \lambda + \vartheta_e) * \cos(r(\alpha - \alpha_n))$$

(4)

Therefore, when a single-phase or a three-phase unit open-circuit fault occurs in the machine, the

magnetomotive force harmonics receive positive and negative harmonic components. Moreover, the $(6r \pm 1)$ component harmonics, which rotate in a positive direction, differ from those rotating in the opposite direction. The generated magnetomotive force is given by

$$f^{rd_k} = f^{rr_k} = -\frac{3f^{r_{\sigma r}}}{2r} = 6r + 3 = 3, 9, 15, 21...$$

$$f^{rd_k} = f^{r_{\sigma r}}, f^{rr_k} = -\frac{3f^{r_{\sigma v}}}{2v} = 6r + 1 = 1, 7, 13, 19, ... \quad (5)$$

$$f^{rd_k} = -\frac{3f^{r_{\sigma r}}}{2r}, f^{rr_k} = f^{r_{\sigma v}} = 6r - 1 = 5, 11, 17, 23, ...$$

Similarly, the rotor's generated magnetomotive force harmonics is given by the following equation

$$f_{Rotor}(\alpha, t) = \sum_{\mu=1}^{\infty} \cos\left(\mu p\alpha \pm \omega_\mu t + \varphi_\mu\right) \quad (6)$$

$f_{r_\mu}$ Represents the coefficient of the rotor's magnetomotive force harmonic $\mu_{th}$ component, while the rotor's angular frequency is given by $\omega_\mu$.

## 3.2 Radial Force Density Distribution of the Prototype Machine

The Maxwell stress tensor method can calculate electric machine radial force density. According to the Maxwell stress tensor method, the radial force density is given by the following equation

$$P_{rad}(\alpha, t) \approx \frac{B_{rad}^2}{2\mu_0} = \frac{B_{rad_S}^2 + 2B_{rad_S}B_{rad_R} + B_{rad_R}^2}{2} \quad (7)$$

Here $B_{rad_S}$ represents the stator radial flux density while $B_{rad_R}$ represents the radial magnetic flux density due to the rotor and are represented by the following equations.

$$B_{rad_S}(\alpha, t) = \sum_{v=1}^{\infty} B_{rad_{v1}} \cos(\omega t - vp\alpha) + B_{rad_{v2}} \cos(\omega t - vp\alpha) \quad (8)$$

$$B_{rad_R}(\alpha, t) = \sum_{\mu=1}^{\infty} B_{rad_\mu} \cos(\mu p\alpha \pm \omega_\mu t + \varphi_\mu) \quad (9)$$

Three components of an electric machine contribute to generating the total electromagnetic force density. These three contributing components come from the stator windings, the permanent magnets and the mutual interaction between the stator windings, and the permanent magnets, expressed by the following equations

$$P_{rad_{vv}}(\alpha, t) = \frac{B_{rad_{sv}}^2}{2\mu_0}(\alpha, t)$$
$$= \frac{1}{4\mu_0}[B_{rad_{sv1}}^2(1 + \cos(2vp\alpha - 2\omega t))$$
$$+ B_{rad_{sv2}}^2(1 + \cos(2vp\alpha - 2\omega t)) + 2B_{rad_{sv1}}B_{rad_{sv2}}(\cos(2vp\alpha)$$
$$+ \cos(2\omega t))] \quad (10)$$

$$P_{rad_{\mu\mu}}(\alpha, t) = \frac{B_{rad_{R\mu}}^2}{2\mu_0}(\alpha, t)$$
$$= \frac{1}{4\mu_0}[B_{rad_\mu}^2(1 + \cos(2\mu p\alpha \pm 2\omega_\mu t + 2\varphi_\mu))] \quad (11)$$

$$P_{rad_{v\mu}}(\alpha, t) = \frac{B_{rad_{sv}}^2(\alpha, t) + B_{rad_{R\mu}}^2(\alpha, t)}{\mu_0}$$
$$= \frac{1}{2\mu_0}[(B_{rad_{sv}}B_{rad_{R\mu}}\cos((v+\mu)p\alpha - (\omega \pm \omega_\mu t) + \varphi_\mu)$$
$$+ B_{rad_{sv}}B_{rad_{R\mu}}\cos((v-\mu)p\alpha - (\omega \pm \omega_\mu t) + \varphi_\mu)$$
$$+ B_{rad_{sv}}B_{rad_{R\mu}}\cos((v+\mu)p\alpha + (\omega \pm \omega_\mu t) + \varphi_\mu)$$
$$+ B_{rad_{sv}}B_{rad_{R\mu}}\cos((v+\mu)p\alpha + (\omega \pm \omega_\mu t) - \varphi_\mu)] \quad (12)$$

Equations (10), (11), and (12) represent the radial force due to the permanent magnet along with the radial force due to the armature windings and the mutual interaction between the (PM) and the stator's armature components.

## 4 Fault-tolerant Operation Under Open Circuit Condition

The modular type fractional slot interior permanent magnet synchronous machine in Fig. 1 has 18 slots 12 poles with a double layer winding configuration. This modular prototype design consists of six-three-phase unit motors with three slots and a pole pair making one three-phase unit motor. Each three-phase unit motor consists of an independent three-phase supply winding. This modular prototype design presented in Fig. 1 has been used to investigate different types of open-circuit faults while ensuring suitable operating reliability.

In a three-phase machine, the winding currents in the stator have a phase shift of 120 electrical degrees, resulting in a circular magnetomotive force driving the machine. Open-circuit faults can be in a single-phase or more than one phase. When a single-phase coil is in an open-circuit fault condition, a phase shift of 180 electrical degrees between the remaining two phases results in a fluctuating (MMF), not suitable for a steady-state generated torque. Similarly, a normal three-phase machine cannot work when two phases

have an open-circuit condition. A modular design machine has the capability to cut off the faulty three-phase unit. The two-phase open-circuit fault condition in a modular design machine can occur in a single three-phase unit, in an adjacent three-phase unit, or it may occur in non-adjacent three-phase units. The various types of three-phase open-circuit faults occurring in a modular design machine are grouped into two main types: symmetrical and asymmetrical faults. Details of the different types of three-phase units open-circuit faults are shown in Fig. 2. Moreover, the distribution of electromagnetic force density is quite different for both types of these open-circuit fault conditions as each unit motor occupies $1/6_{th}$ of the machine's circumferential space. Also, the magnetic force density is spread around the complete circumference of the machine; hence the modular design machine vibration characteristic is quite different for both cases.

## 4.1 Radial Force Density of the Prototype Machine with Associated Harmonics

The electromagnetic field distribution in the modular type machine design is very different for the symmetrical and asymmetrical three-phase units open circuit fault conditions; subsequently, the resulting distribution of radial electromagnetic force density inside the machine air gap is also quite different. Results from Figs. 3, 4, 5 show the radial force density distribution for the modular prototype machine with
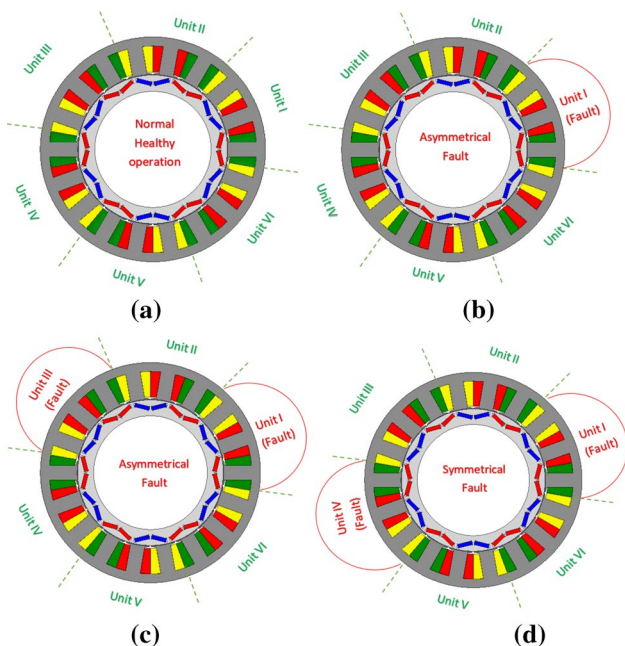


(a)



(b)

**Fig. 3** Machine's healthy operating conditions **a** Radial force density waveform **b** Harmonic components of the machine radial force density under healthy conditions

the associated time and space harmonic contents for the different operating cases. The corresponding time and space harmonics for the modular type design machine are obtained using two-dimensional Fast Fourier Transform (FFT). Figure 3a and b show the radial force density and its time and space harmonics for the normal healthy case when all the three-phase units work synchronously without any fault. Similarly, Fig. 4a and b show the radial force density waveform and its time and space harmonics under asymmetrical fault operating conditions when unit motor I and unit motor III are in the open-circuit operating conditions by cutting up the supply to these three-phase units of the prototype modular design machine. Low-order sub-harmonics can be seen in this kind of operating condition. By comparing the machine's healthy operating condition and the asymmetrical fault with two three-phase unit failures, low order sub-harmonics are induced for the two asymmetrical three-phase



**Fig. 2** Modular design of IPMSM **a** Normal healthy condition **b** Single three-phase unit fault (Asymmetrical) **c** Two three-phase units fault (Asymmetrical) **d** Two three-phase units fault (Symmetrical)
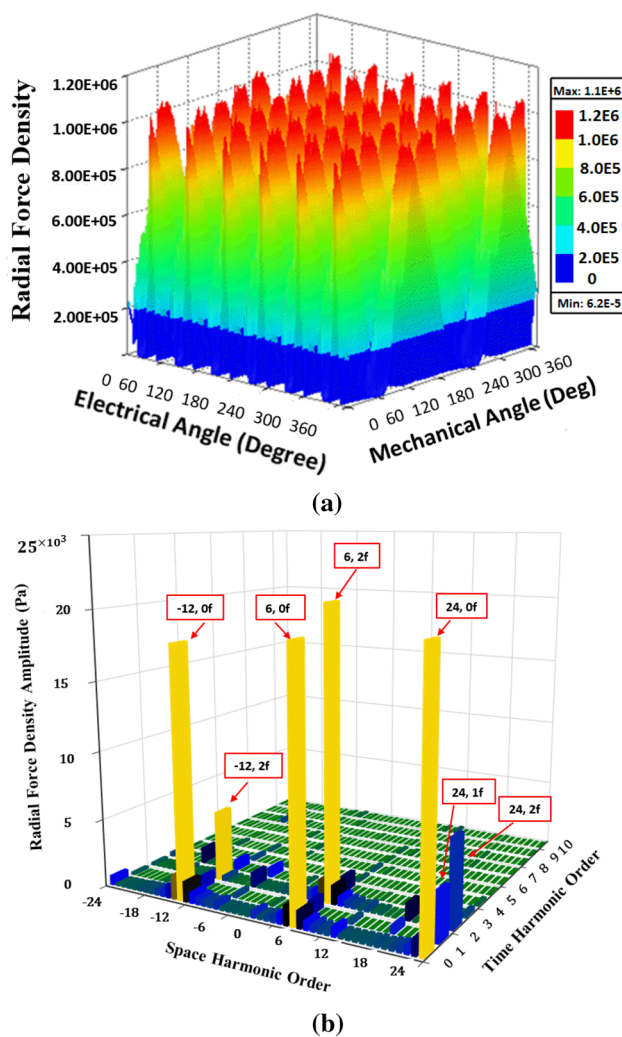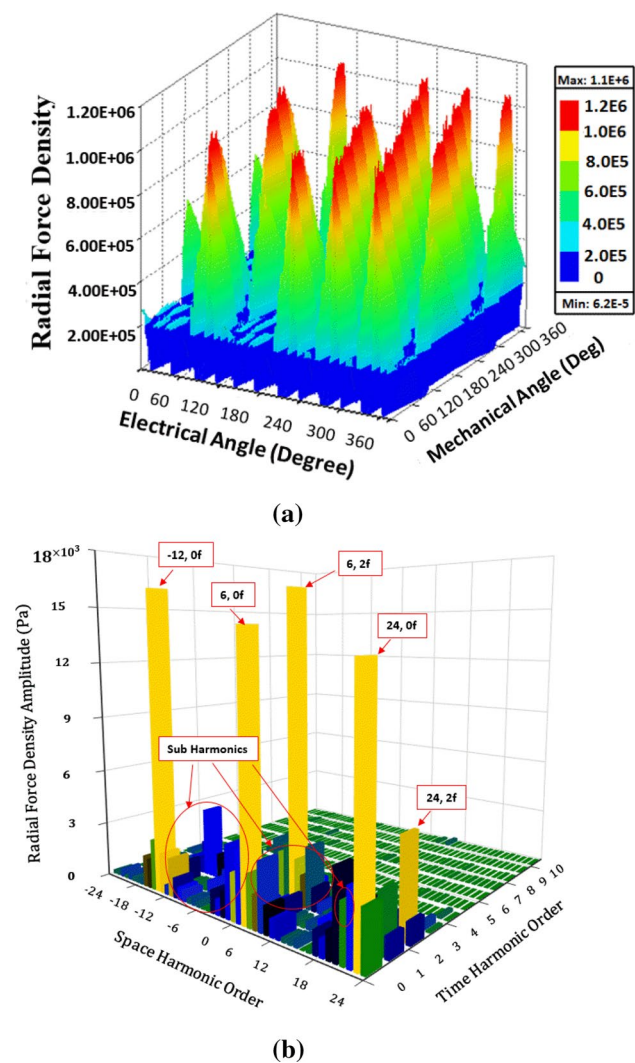
**(a)**



**(b)**

**Fig. 4** Machine's three-phase units fault opertaions **a** The waveform of radial force density under two units fault (asymmetric) **b** Harmonic contents of radial force density under two units fault (asymmetric) condition



**(a)**



**(b)**

**Fig. 5** **a** Waveform of radial force density under two units fault (symmetric) condition **b** Harmonic contents of radial force density under two units fault (symmetric) condition

unit motors fault conditions. These sub-harmonics are much higher in number and amplitude than the healthy operating condition, for which case they are almost negligible. These observations are illustrated in Table 2, presenting the amplitudes of the main harmonics and the induced sub-harmonics for both the operating conditions. The values of the harmonic amplitudes inside square brackets represent the condition when both the radial and tangential components of the electromagnetic force density are taken into consideration, while the values without brackets represent only the radial component ignoring the tangential component of electromagnetic force density.

One more case of symmetrical fault operating conditions is studied when the power supply is cut off to two symmetric three-phase unit motors I and IV, resulting in an open-circuit
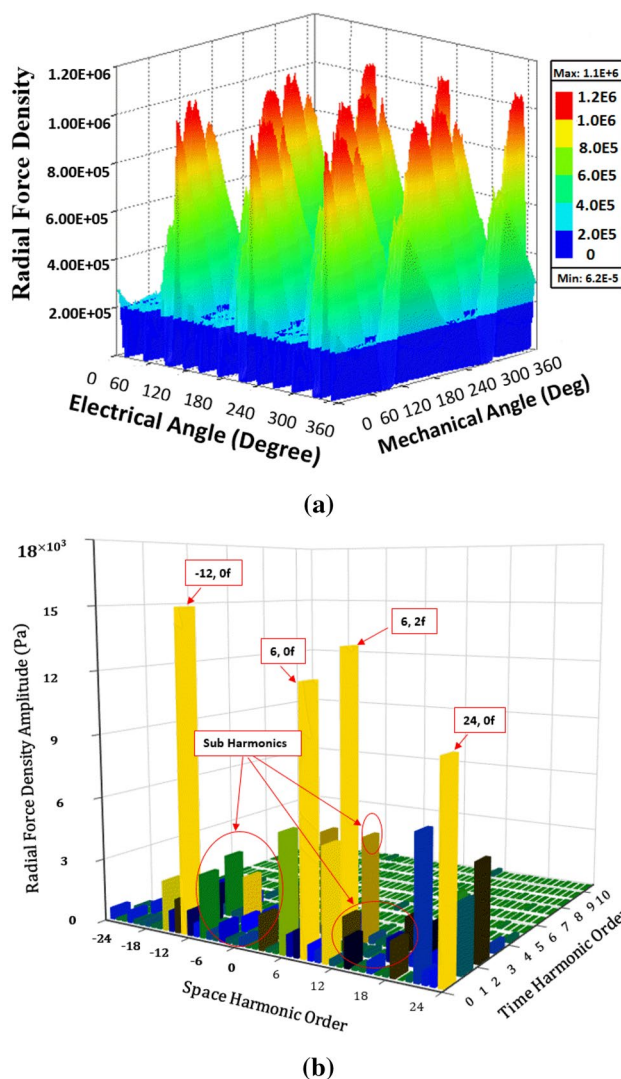
fault condition in these units. Figure 5a and b show the radial force density waveform and its time and space harmonics for the symmetrical faulty condition. Table 2 shows the amplitudes of the main harmonics and the induced sub-harmonics for the machine healthy and the symmetrical fault operating conditions.

Under the symmetric open-circuit fault condition, low order sub-harmonics are also generated in the radial force density of the machine. There is no considerable difference in the amplitude of the machine radial force density main harmonic components for the asymmetric and symmetric three-phase units fault operating conditions. However, the amplitudes of the low order sub-harmonics are quite different for both three-phase units' fault operating conditions. The (0f,2f,4f) sub-harmonic components are comparatively

**Table 2** Comparison of main electromagnetic force density harmonics and sub-harmonics under healthy, asymmetric, and symmetric three-phase units faulty conditions

| Harmonic order | Amplitudes of radial force density components (N/m$^2$) | | |
|---|---|---|---|
| | Normal healthy operation | Asymmetrical faulty operation | Symmetrical faulty operation |
| (0, 2f) | 301 [251] | 577 | 985 |
| (6, 0f) | 18823 [19198] | 16,354 | 12,003 |
| (6, 2f) | 20793 [21324] | 18,340 | 13,292 |
| (6, −2f) | 1120 [1151] | 860 | 603 |
| (12, 0f) | 696 [692] | 595 | 1362 |
| (12, −2f) | 5139 [4601] | 4448 | 2967 |
| *Sub-harmonics* | | | |
| (2, 0f) | 383 | 1213 | 109 |
| (2, 2f) | 340 | 1324 | 341 |
| (3, 0f) | 464 | 3730 | 5467 |
| (3, 2f) | 513 | 3205 | 4815 |
| (4, 0f) | 789 | 2437 | 987 |
| (4, 2f) | 788 | 2547 | 734 |

higher for the asymmetrical three-phase unit fault than the symmetrical three-phase unit fault conditions. Henceforth, they have more effect on the vibration and noise behavior of the prototype machine under three-phase unit fault operating conditions.

Similarly, the induced low order sub-harmonics are more crowded for the asymmetrical three-phase unit fault case. In contrast, those under the symmetrical three-phase units' faulty condition are more spread out. The difference between the amplitude of the harmonics in the radial force density for the dominant components and the low order sub-harmonic components under asymmetrical and symmetrical faulty operating conditions are shown in Table 2.

## 5 Structural and Vibration Response Analyses Under Three-phase Units Open Circuit Condition

### 5.1 Structural Response Analysis

A 3D structural response analysis of the machine's stator core is investigated using the structural finite element analysis, knowing the radial force density distribution on each stator teeth under symmetrical and asymmetrical three-phase units open-circuit fault cases. The structural finite element analysis investigates the machine's stator core total deformation and the stress distribution under both symmetrical and asymmetrical fault conditions. The maximum deformation of the machine's stator core under asymmetrical and symmetrical two three-phase unit faults are shown in Fig. 6a and b, respectively.
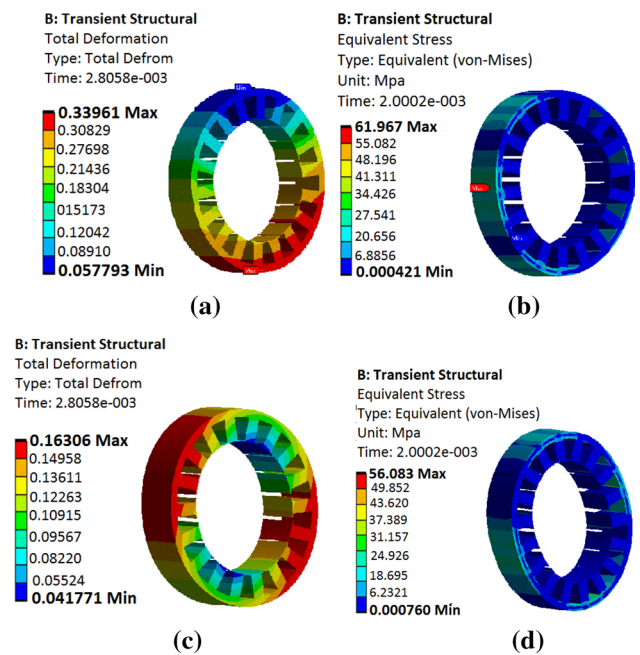


**Fig. 6** Stator structure analysis **a**. Maximum deformation (asymmetrical case) **b** Maximum stress (asymmetrical case) **c** Maximum deformation (symmetrical case) **d** Maximum stress (symmetrical case)

Similarly, Fig. 6b and d show the maximum stress on the stator core under the asymmetrical and symmetrical two three-phase unit fault operating condition. Table 3 compares the maximum deformation and stress response analysis of the machine's stator core under two three-phase units, symmetrical and asymmetrical fault cases.

The machine's stator core maximum deformation for the asymmetrical two three-phase unit fault is 107.2% higher

**Table 3** 3D-Structural analysis of the machine's stator

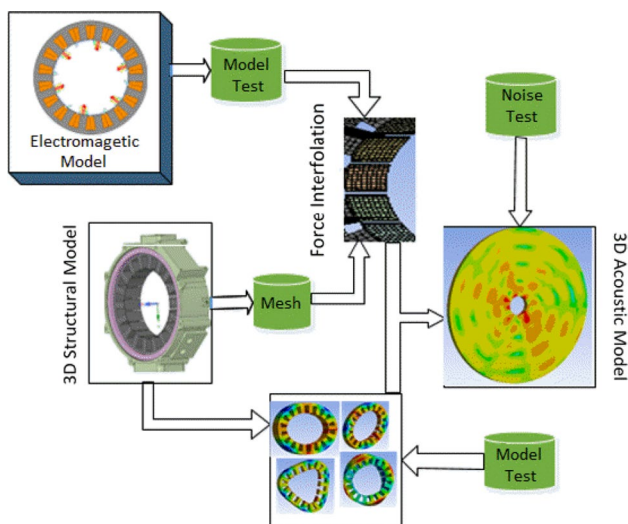| Modular type multi three-phase machine | 3D structural behavior of Stator core | | |
|---|---|---|---|
| | Asymmetrical two three-phase unit fault | Symmetrical two three-phase unit fault | % difference |
| Maximum deformation (mm) | 0.339 | 0.163 | 107.2% |
| Maximum deformation (mm) | 61.967 | 56.083 | 10.5% |



**Fig. 7** Flowchart to represent the process for the calculation of machine vibration and noise



**Fig. 8** The noise spectrum for a normal healthy condition and asymmetrical two three-phase units fault

than the symmetrical two three-phase units fault. Similarly, the maximum stress for an asymmetrical fault condition on the stator core is 10.5% higher than the symmetrical two three-phase unit fault.

## 5.2 Noise and Vibration Response Analysis

The vibration and noise behavior of the modular prototype IPMSM machine under post fault operating conditions is investigated through a multi-physics analysis. The established multi-physics model with a detailed analysis flowchart is shown in Fig. 7.

The multi-physics analysis starts with calculating the nodal forces acting on the teeth surface of the stator slots based on the electromagnetic (2D) FEA model of the prototype machine. The nodal forces are mapped to the machine's structural model as an excitation source. Lastly, the machine's model noise and vibration response are calculated using the modal superposition method. The modal superposition method (MSM) uses the following equation for vibration response analysis

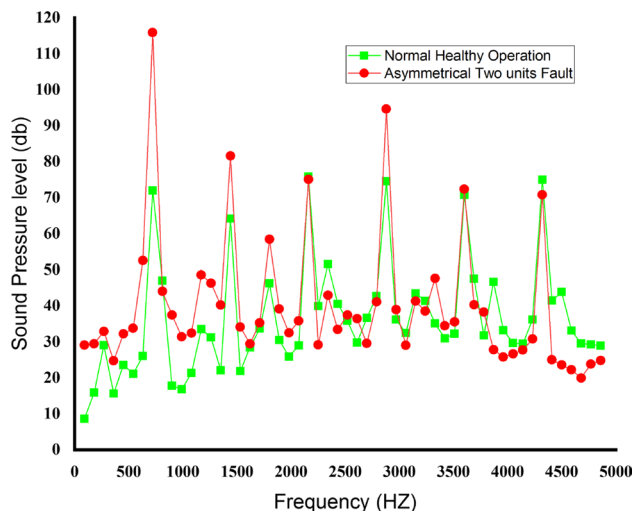$$[M] \sum_i^N \{\varphi_i\}\ddot{y}_i + [C] \sum_i^N \{\varphi_i\}\dot{y}_i + [K] \sum_i^N \{\varphi_i\}y_i = [F]$$

Here $y_i$ is the forced response and can be written as the sum of the superposition of the modes.

$$y_i = \sum_i^N \{\varphi_i\}\eta_i$$

The noise response of the prototype modular design machine is presented next to investigate the noise behavior of the modular type machine and their mechanical system. The corresponding noise response is investigated using the multi-physic model analysis. Based on the multi-physics model analysis, the generated sound pressure level for the asymmetric and symmetric three-phase units faulty conditions is investigated, respectively.

### 5.2.1 Noise Response Analysis Under Two Three-phase Units Asymmetrical Fault

Firstly, the noise response analysis for both the normal healthy operating machine and an asymmetrical two three-phase units' faulty condition is investigated thoroughly. A detailed multi-rpm analysis is conducted to further investigate the faulty operating machine condition under different speed ranges to observe the machine vibration and noise

behavior. Figure 8 shows the plot of the noise spectrum under normal healthy and two three-phase units asymmetrical fault conditions.

It can be seen from the noise spectrum plot presented by Fig. 8 that the machine sound pressure level (SPL) under an asymmetric faulty condition is quite higher at the low-frequency range compared to the healthy operating condition of the machine. This increase in the machine noise level is due to the induction of low order sub-harmonics, especially at (2f and 4f) harmonic frequency under an asymmetrical fault condition.

Furthermore, a multi-speed range noise analysis of the asymmetrical two three-phase unit fault is conducted. Figure 9 shows the multi-speed range analysis representing the equivalent radiated power level for the two three-phase units asymmetrical fault condition. The corresponding plot illustrates lower radiated power levels at 1800 and 2400 rpm than the rated speed operation at 3600 rpm.

### 5.2.2 Noise Response Analysis Under Two Symmetrical Three-phase Units Fault

Two three-phase units fault is introduced in the machine by cutting up the supply to two three-phase units symmetrically distributed around the machine's circumference. It investigates the machine's noise response under symmetrical three-phase units fault conditions. The noise spectrum analysis plot of the two three-phase units under symmetrical fault conditions and normal healthy operating conditions of the machine is shown in Fig. 10. The corresponding comparative analysis plot shows the machine sound pressure level (SPL) in a healthy normal operating condition and under symmetrical two three-phase units fault of the machine prototype.

It can be observed from the comparison plots presented in Fig. 10 that the sound pressure level (SPL) is much higher
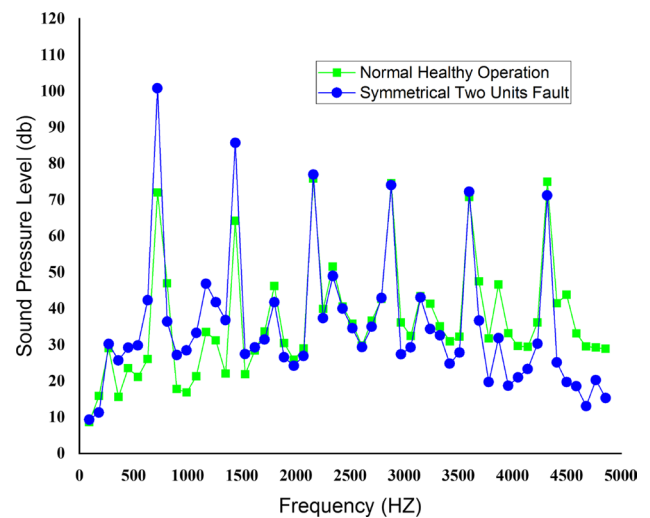


**Fig. 10** The noise spectrum for normal healthy conditions and symmetrical two three-phase units fault

for the symmetrical two three-phase units fault operating conditions than the machine's normal healthy operating condition.

The multi-speed range analysis representing the equivalent radiated power level for two three-phase units symmetrical fault conditions is shown in Fig. 11. The corresponding plot illustrates a lower radiated power level at a speed of 3000 rpm and a rated speed of 3600 rpm compared to the other analyzed speed range.

### 5.3 Comparison Between Symmetrical and Asymmetrical Two Three-phase Units Fault

A comparative analysis of the symmetrical and asymmetrical three-phase units' faulty condition is conducted in this
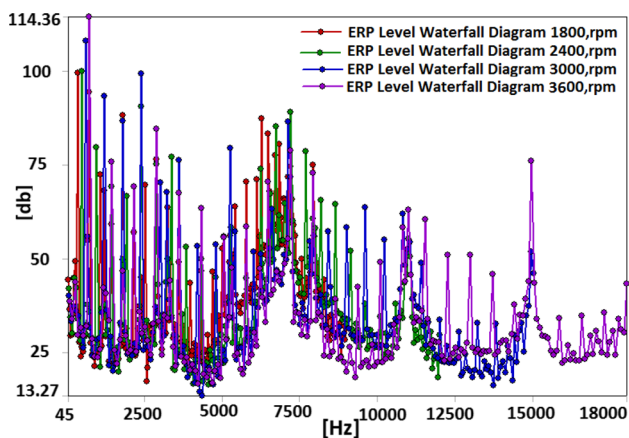


**Fig. 9** Equivalent Radiated Power level with multi-speed range under two asymmetrical three-phase units fault
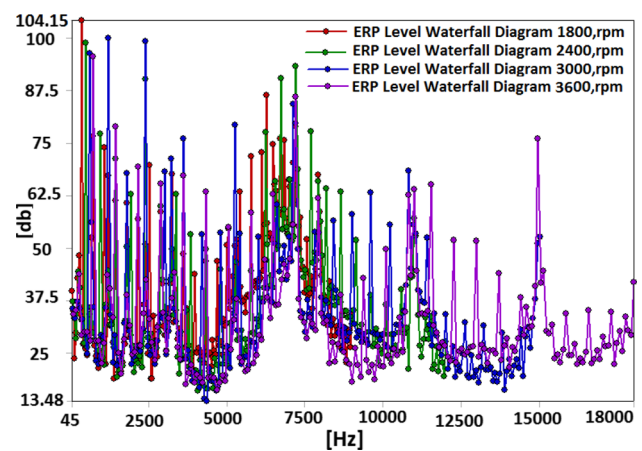


**Fig. 11** Equivalent Radiated Power level with multi-speed range under two symmetrical three-phase units fault
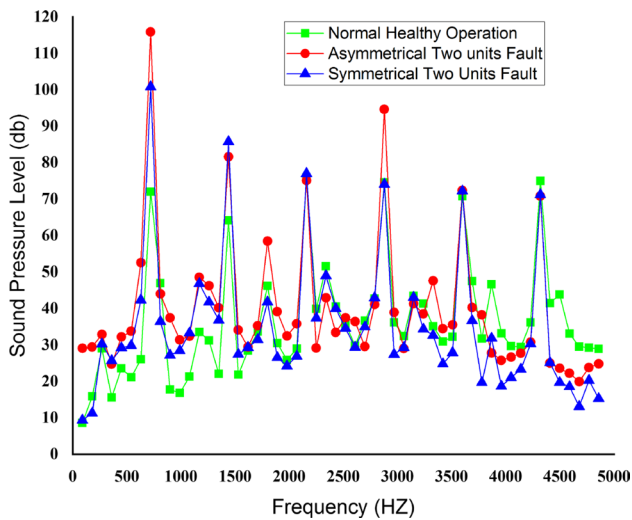
**Fig. 12** Noise spectrum plot for the machine's normal healthy condition and for two three-phase units asymmetrical and symmetrical fault conditions



**Fig. 13** The stator winding of multi three-phase unit machine **a** Winding process **b** Stator winding connections



**Fig. 14** Experimental platform to measure the vibration response of the multi three-phase prototype (IPMSM)
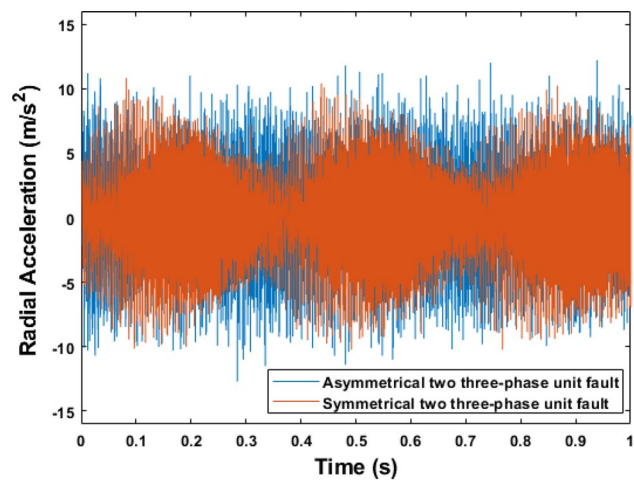


**Fig. 15** Measured vibration waveform for an asymmetrical and symmetrical two three-phase unit fault in the machine

section. The corresponding noise spectrum plot for two three-phase units symmetrical and an asymmetrical fault is shown in Fig. 12. It can be seen clearly from the noise spectrum plot that the corresponding sound pressure level is comparatively higher for an asymmetrical three-phase units fault condition compared to symmetrical three-phase units fault condition.

# 6 Experimental Validation

A 35kw modular type (IPMSM) prototype machine is used to experimentally verify the asymmetrical and symmetrical three-phase units faults and validate their effect on the machine's vibration and noise level. Figure 13a–b shows the stator winding arrangement design process for the prototype six three-phase units machine.

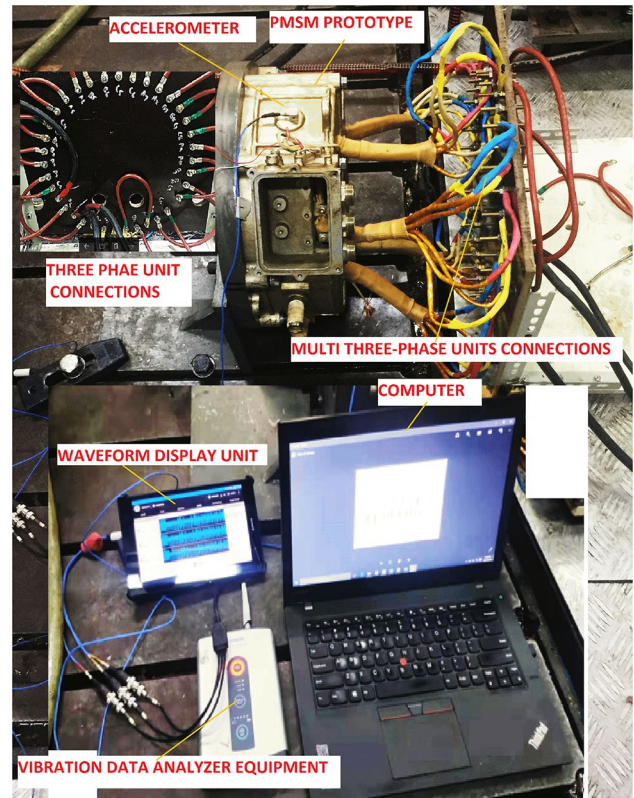The experimental setup used in the analysis is shown in Fig. 14. An accelerometer is placed at a specific point to measure the vibration of the machine in the radial direction for the asymmetrical and symmetrical three-phase units fault operating conditions. The experimental procedure is repeated for both the fault operating conditions under the same operating condition (Fig. 15).
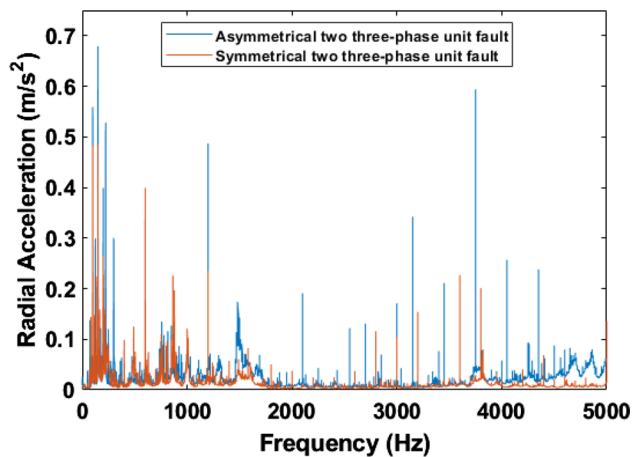
**Fig. 16** Vibration spectrum for an asymmetrical and symmetrical two three-phase unit fault in the machine

The comparative analysis of the radial acceleration waveform shows that the generated vibration level for the symmetrical two three-phase unit fault operating condition is smaller compared to the asymmetrical fault operating condition validating the analysis presented. The radial vibration spectrum plot comparison is shown in Fig. 16 for the fault operating conditions. The corresponding vibration spectrum plot shows that the asymmetrical three-phase unit fault operating conditions bring a high vibration level due to the induction of a higher level of sub-harmonic components compared to the symmetrical three-phase unit fault condition.

# 7 Conclusion

This paper presents a detailed investigation of the radial electromagnetic forces, vibration, and noise behavior of a modular type designed (IPM) synchronous machine under normal, symmetrical, and asymmetrical three-phase units open-circuit fault operating conditions. First theoretical analysis for the different open circuit fault conditions is discussed, then a comprehensive simulation based on the finite element analysis along with a detailed experimental validation is performed on a 35kw (IPMSM) to verify the results. The different findings from the analyses confirm a high level of radial force density sub-harmonics induced for three-phase unit open-circuit fault cases compared to the healthy operating condition of the modular prototype machine. Moreover, for the case of an asymmetrical three-phase units fault condition, the induced low order sub-harmonics are more crowded together than the symmetrical three-phase unit fault operating condition. These low-order sub-harmonics are more spread out for symmetrical three-phase units fault conditions. By applying (2-D) (FFT) analysis, the

harmonic response waveform and spectral response analysis are obtained for the three-phase unit fault operating cases. The corresponding harmonic response analysis for both the fault operating conditions confirms large, crowded, and rich low order sub-harmonics for asymmetric three-phase unit fault operating conditions compared to the symmetrical three-phase unit fault operating conditions.

Similarly, the (3-D) structural response analysis confirms that the corresponding deformation and applied stress on the machine stator core are higher for the asymmetric three-phase unit fault condition than the symmetrical three-phase fault operating condition. The noise and vibration comparative analysis confirms rich low order sub-harmonics for both types of three-phase units fault cases. However, the amplitudes of these sub-harmonics are more intense, resulting in a greater vibration level for the modular prototype machine with asymmetrical three-phase fault than the same machine with symmetrical three-phase unit fault, confirmed by experimental investigations. The noise and vibration analysis work presented in this paper can be used further for the noise and vibration reduction in multi three-phase machines for fault-tolerant applications.

# References

1. Wang J, Xia ZP, Long SA, Howe D (2006) Radial force density and vibration characteristics of modular permanent magnet brushless AC machine. Proc Inst Elect Eng Electr Power Appl 153(6):793–801
2. Lin C, Wang S, Moallem M, Fahimi B, Tschida C (2017) Analysis of vibration in permanent magnet synchronous machines due to variable speed drives. IEEE Trans Energy Conv 32(2):582–590
3. Besnerais JL (2015) Vibroacoustic analysis of radial and tangential airgap magnetic forces in permanent magnet synchronous machines. IEEE Trans Magn 51(6):1–9
4. Valavi M, Le Besnerais J, Nysveen A (2016) An investigation of zeroth-order radial magnetic forces in low-speed surface-mounted permanent magnet machines. IEEE Trans Magn 52(8):1–6
5. Ebrahimi H, Gao Y, Dozono H, Muramatsu K, Okitsu T, Matsuhashi D (2016) Effects of stress and magnetostriction on loss and vibration characteristics of motor. IEEE Trans Magn 52(3):1–4
6. Valavi M, Nysveen A, Nilssen R (2015) Effects of loading and slot harmonic on radial magnetic forces in low-speed permanent magnet machine with concentrated windings. IEEE Trans Magn 51(6):1–10
7. Verez G, Barakat G, Amara Y et al (2015) Impact of pole and slot combination on vibrations and noise of electromagnetic origins in permanent magnet synchronous motors. IEEE Trans Magn 51(3):1–4
8. Lin F, Zuo S, Wu X (2016) Electromagnetic vibration and noise analysis of permanent magnet synchronous motor with different slot pole combinations. IET Electr Power Appl 10(9):900–908
9. Gan C, Wu J, Shen M, Yang S, Hu Y, Cao W (2015) Investigation of skewing effects on the vibration reduction of three-phase switched reluctance motors. IEEE Trans Magn 51(9):1–9
10. Wang J, Xia ZP, Howe D, Long SA (2006) Vibration characteristics of modular permanent magnet brushless AC machines. In:

Conference record of the 2006 IEEE industry applications conference forty-first IAS annual meeting, vol 3, pp 1501–1506

11. Sui Y, Zheng P, Wu F, Wang P, Cheng L, Zhu J (2015) A novel five phase fault-tolerant modular in-wheel permanent-magnet synchronous machine for electric vehicles. J Appl Phys 117:17B521

12. Sun T, Kim J-M, Lee G-H, Hong J-P, Choi M-R (2011) Effect of pole and slot combination on noise and vibration in permanent magnet synchronous motor. IEEE Trans Magn 47(5):1038–1041

13. Gao P, Gu Y, Shah SH, Abubakar U, Wang X (2019) Calculation and analysis of flux leakage coefficient of interior permanent magnet synchronous motors with fractional slot concentrated windings. IEEE Trans Appl Supercond 29(2):1–4

14. Wang X, Sun X, Gao P (2019) Study on the effects of rotor-step skewing on the vibration and noise of a PMSM for electric vehicles. IET Electr Power Appl 14(1):131–138

15. Deng W, Zuo S (2019) Electromagnetic vibration and noise of the permanent-magnet synchronous motors for electric vehicles: an overview. IEEE Trans Transp Electrification 5(1):59–70. https://doi.org/10.1109/TTE.2018.2875481

16. Shah SH et al (2021) Investigation of noise and vibration characteristics of an IPMSM with modular-type winding arrangements having three-phase sub-modules for fault-tolerant applications. IET Electr Power Appl. https://doi.org/10.1049/elp2.12150

**Usman Abubakar** was born in Kano state, Nigeria. He obtained B.Eng, and M.Eng.degrees in electrical engineering from Kano University ofScience and Technology, Wudil, Nigeria, in 2011 andLiaoning University of Technology, Jinzhou, China, in 2014,respectively. He is pursuing a Ph.D. degree in E lectricalengineering at Tianjin University. His research interestsinclude the design of a cooling system and thermal analysisof high speed PMSM.



**Peng Gao** was born in Hebei,China, in 1985. He received the B.Eng. In electricalengineering from the Shenyang University of ChemicalTechnology, Shenyang, China, in 2009, and the M.Sc. andPh.D. degrees in Electrical E ngineering from TianjinUniversity, Tianjin, China, in 2011 and 2015, respectively.He has been serving as assistant Professor at the School ofElectrical and Information Engineering, Tianjin University.His research interests include E lectrical machines designand motor drives system for high speed applications.



**Sayyed Haleem Shah** was born inIslamabad, Pakistan. He received his B.Sc. and M.S. degreein Electrical Engineering from the University ofEngineering and Technology, Peshawar, Pakistan, in 2011and Air University, Islamabad, Pakistan, in 2014,respectively. He is currently pursuing Ph.D. degree inElectrical E ngineering at the School of Electrical andInformation Engineering, Tianjin University, China. Hisresear ch interests include design of E lectrical machines,modular type machines, noise and vibration in modular typemachines.



**Xiaoyuan Wang** was born in Hebei,China, in 1962. He received the B.S. and M.S. degrees inElectrical Engineering from Tianjin University, Tianjin,China, in 1982 and 1985, respectively, and the Ph.D. degreein Electrical Engineering from Shenya ng University ofTechnology, Shenyang, China, in 2006. He has been servingas Professor at the School of Electrical and InformationEngineering, Tianjin University, since 2007. His curr entresearch interests include E lectrical machine design, motordrive s ystem for electric vehicles for high speedapplications.